

Non-perturbative three-nucleon simulation using chiral lattice EFT

Lukas Bovermann (lukas.bovermann@rub.de),
E. Epelbaum, H. Krebs, D. Lee
— code contribution by S. Elhatisari —

Institut für Theoretische Physik II
Ruhr-Universität Bochum

RUHR
UNIVERSITÄT
BOCHUM



The 11th International Workshop
on Chiral Dynamics



Ruhr-Universität Bochum, Germany
26-30 August 2024

Outline

1 Chiral lattice interaction

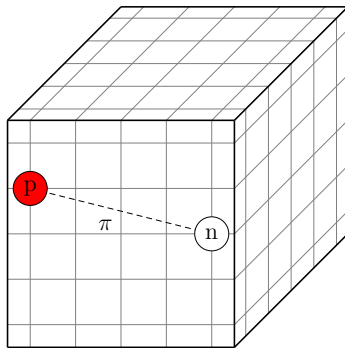
2 Three-nucleon results

- Binding energies
- Charge radii
- Half-life

3 Summary and outlook

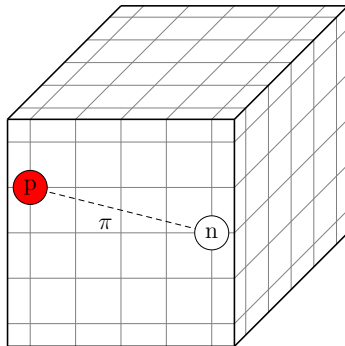
Lattice definition

- work with nucleons & pions (\neq lattice QCD)

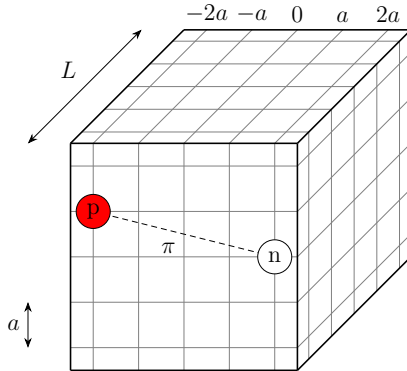


Lattice definition

- work with nucleons & pions (\neq lattice QCD)
- no Monte Carlo (MC) & perturbation theory for 3 nucleons [see plenary talk by D. Lee for many-body case](#)

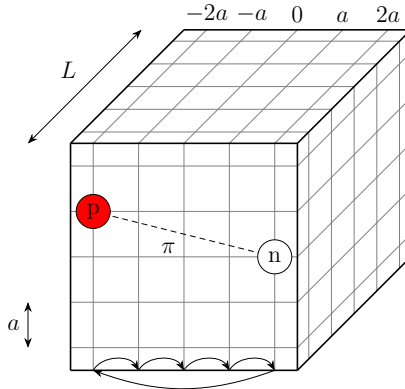


Lattice definition



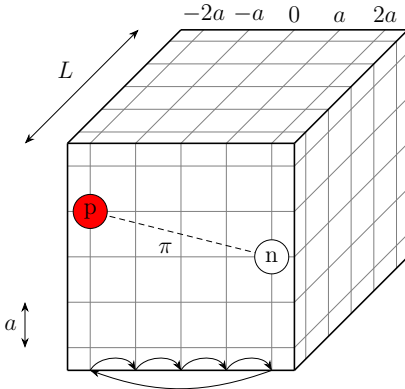
- work with nucleons & pions (\neq lattice QCD)
- no Monte Carlo (MC) & perturbation theory for 3 nucleons [see plenary talk by D. Lee for many-body case](#)
- introduce lattice with length L and spacing $a = 2 \text{ fm}$

Lattice definition



- work with nucleons & pions (\neq lattice QCD)
- no Monte Carlo (MC) & perturbation theory for 3 nucleons [see plenary talk by D. Lee for many-body case](#)
- introduce lattice with length L and spacing $a = 2 \text{ fm}$
- require periodic boundary conditions:
$$|\vec{r}\rangle = |\vec{r} + n_x L \vec{e}_x + n_y L \vec{e}_y + n_z L \vec{e}_z\rangle$$
$$\forall n_x, n_y, n_z \in \mathbb{Z}$$

Lattice definition



improved version of

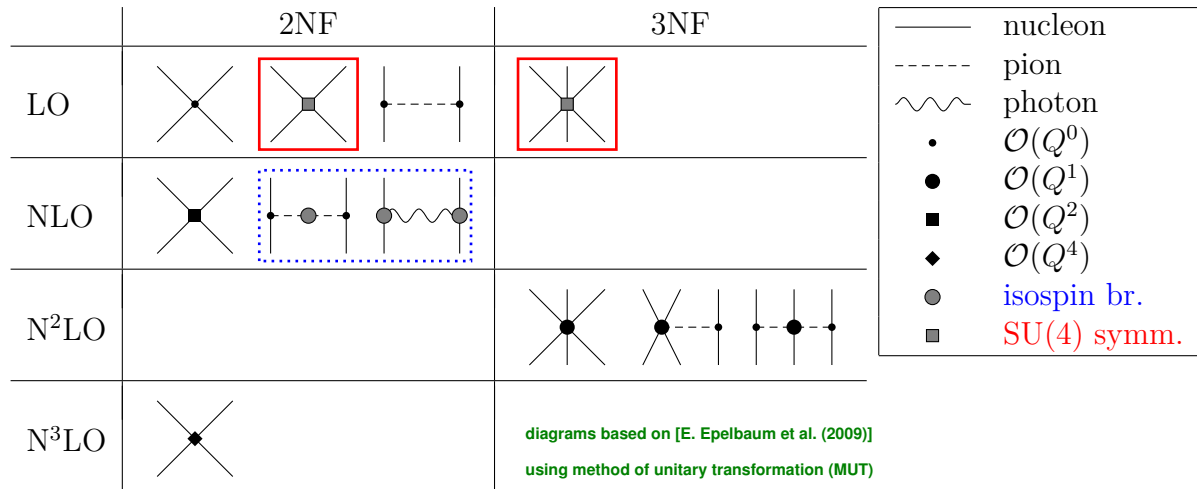
$$-\frac{\vec{\nabla}^2}{2m_N} |\vec{r}\rangle = \frac{3}{m_N a^2} |\vec{r}\rangle - \frac{1}{2m_N a^2} \sum_{i=x,y,z} \left(|\vec{r} + a\vec{e}_i\rangle + |\vec{r} - a\vec{e}_i\rangle \right)$$

- work with nucleons & pions (\neq lattice QCD)
- no Monte Carlo (MC) & perturbation theory for 3 nucleons [see plenary talk by D. Lee for many-body case](#)
- introduce lattice with length L and spacing $a = 2$ fm
- require periodic boundary conditions:
 $|\vec{r}\rangle = |\vec{r} + n_x L \vec{e}_x + n_y L \vec{e}_y + n_z L \vec{e}_z\rangle$
 $\forall n_x, n_y, n_z \in \mathbb{Z}$
- discretize integrals and derivatives, e.g. for kinetic energy in \hat{H} : [\[D. Lee, R. Thomson \(2007\)\]](#)

Chiral expansion of nuclear force

	2NF	3NF	
LO			
NLO	 		
N ² LO			
N ³ LO			<p>diagrams based on [E. Epelbaum et al. (2009)] using method of unitary transformation (MUT)</p>

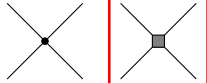
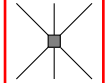
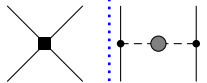
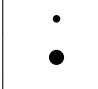
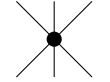
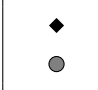
Chiral expansion of nuclear force



differences to continuum: new contact interactions (Cl's) with Wigner SU(4) symmetry

[N. Li et al. (2018)]

Chiral expansion of nuclear force

	2NF	3NF	
LO			
NLO			
N ² LO			
N ³ LO		<p>diagrams based on [E. Epelbaum et al. (2009)] using method of unitary transformation (MUT)</p>	

differences to continuum: new contact interactions (Clis) with Wigner SU(4) symmetry

[N. Li et al. (2018)]

no 3π and simultaneous 2π exchange (emulated by Clis)
no relativistic $1/m_N$ corrections

Two-nucleon short-range interactions *[N. Li et al. (2018)]

$$\langle x | \hat{O} | x' \rangle = \begin{pmatrix} 0 & 0 & 0 & 0 & 0 \\ 0 & 0 & 0 & 0 & 0 \\ 0 & 0 & 1 & 0 & 0 \\ 0 & 0 & 0 & 0 & 0 \\ 0 & 0 & 0 & 0 & 0 \end{pmatrix}$$

$x = x' = 0$

(x = 2N coordinate difference in 1D)

Two-nucleon short-range interactions *[N. Li et al. (2018)]

$$\langle x | \hat{O}_{\text{NL}} | x' \rangle = \begin{pmatrix} 0 & 0 & 0 & 0 & 0 \\ 0 & s_{\text{NL}}^2 & s_{\text{NL}} & s_{\text{NL}}^2 & 0 \\ 0 & s_{\text{NL}} & 1 & s_{\text{NL}} & 0 \\ 0 & s_{\text{NL}}^2 & s_{\text{NL}} & s_{\text{NL}}^2 & 0 \\ 0 & 0 & 0 & 0 & 0 \end{pmatrix}$$

$$\langle x | \hat{O}_{\text{L}} | x' \rangle = \begin{pmatrix} 0 & 0 & 0 & 0 & 0 \\ 0 & s_{\text{L}} & 0 & 0 & 0 \\ 0 & 0 & 1 & 0 & 0 \\ 0 & 0 & 0 & s_{\text{L}} & 0 \\ 0 & 0 & 0 & 0 & 0 \end{pmatrix}$$

(x = 2N coordinate difference in 1D)

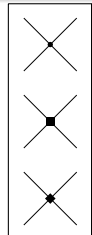
Two-nucleon short-range interactions

*[N. Li et al. (2018)]

- “standard” contact interactions for different partial waves (PWs)

- non-local smearing similar to Gaussian regulator in continuum SMS potential

[P. Reinert et al. (2018)]



$$\langle x | \hat{O}_{NL} | x' \rangle = \begin{pmatrix} 0 & 0 & 0 & 0 & 0 \\ 0 & s_{NL}^2 & s_{NL} & s_{NL}^2 & 0 \\ 0 & s_{NL} & 1 & s_{NL} & 0 \\ 0 & s_{NL}^2 & s_{NL} & s_{NL}^2 & 0 \\ 0 & 0 & 0 & 0 & 0 \end{pmatrix}$$

$$\langle x | \hat{O}_L | x' \rangle = \begin{pmatrix} 0 & 0 & 0 & 0 & 0 \\ 0 & s_L & 0 & 0 & 0 \\ 0 & 0 & 1 & 0 & 0 \\ 0 & 0 & 0 & s_L & 0 \\ 0 & 0 & 0 & 0 & 0 \end{pmatrix}$$

(x = 2N coordinate difference in 1D)

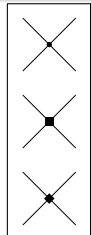
Two-nucleon short-range interactions

*[N. Li et al. (2018)]

- “standard” contact interactions for different partial waves (PWs)

- non-local smearing similar to Gaussian regulator in continuum SMS potential

[P. Reinert et al. (2018)]



$$\langle x | \hat{O}_{NL} | x' \rangle = \begin{pmatrix} 0 & 0 & 0 & 0 & 0 \\ 0 & s_{NL}^2 & s_{NL} & s_{NL}^2 & 0 \\ 0 & s_{NL} & 1 & s_{NL} & 0 \\ 0 & s_{NL}^2 & s_{NL} & s_{NL}^2 & 0 \\ 0 & 0 & 0 & 0 & 0 \end{pmatrix}$$

- SU(4)-invariant CI with coeff. $C_{0,2N}$

- non-local & local smearing



$$\langle x | \hat{O}_L | x' \rangle = \begin{pmatrix} 0 & 0 & 0 & 0 & 0 \\ 0 & s_L & 0 & 0 & 0 \\ 0 & 0 & 1 & 0 & 0 \\ 0 & 0 & 0 & s_L & 0 \\ 0 & 0 & 0 & 0 & 0 \end{pmatrix}$$

(x = 2N coordinate difference in 1D)

Two-nucleon short-range interactions

*[N. Li et al. (2018)]

- “standard” contact interactions for different partial waves (PWs)

- non-local smearing similar to Gaussian regulator in continuum SMS potential

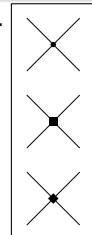
[P. Reinert et al. (2018)]

- MC: treat $N^{n>0}$ LO perturbatively

- SU(4)-invariant CI with coeff. $C_{0,2N}$

- non-local & local smearing

- MC: roughly reproduce $\alpha\alpha$ interaction strength [S. Elhatisari et al. (2016)] at LO non-pert.



$$\langle x | \hat{O}_{NL} | x' \rangle = \begin{pmatrix} 0 & 0 & 0 & 0 & 0 \\ 0 & s_{NL}^2 & s_{NL} & s_{NL}^2 & 0 \\ 0 & s_{NL} & 1 & s_{NL} & 0 \\ 0 & s_{NL}^2 & s_{NL} & s_{NL}^2 & 0 \\ 0 & 0 & 0 & 0 & 0 \end{pmatrix}$$

$$\langle x | \hat{O}_L | x' \rangle = \begin{pmatrix} 0 & 0 & 0 & 0 & 0 \\ 0 & s_L & 0 & 0 & 0 \\ 0 & 0 & 1 & 0 & 0 \\ 0 & 0 & 0 & s_L & 0 \\ 0 & 0 & 0 & 0 & 0 \end{pmatrix}$$

($x = 2N$ coordinate difference in 1D)

Two-nucleon short-range interactions

*[N. Li et al. (2018)]

- “standard” contact interactions for different partial waves (PWs)

- non-local smearing similar to Gaussian regulator in continuum SMS potential

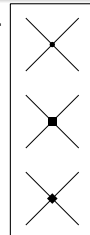
[P. Reinert et al. (2018)]

- MC: treat $N^{n>0}$ LO perturbatively

- SU(4)-invariant CI with coeff. $C_{0,2N}$

- non-local & local smearing

- MC: roughly reproduce $\alpha\alpha$ interaction strength [S. Elhatisari et al. (2016)] at LO non-pert.



$$\langle x | \hat{O}_{NL} | x' \rangle = \begin{pmatrix} 0 & 0 & 0 & 0 & 0 \\ 0 & s_{NL}^2 & s_{NL} & s_{NL}^2 & 0 \\ 0 & s_{NL} & 1 & s_{NL} & 0 \\ 0 & s_{NL}^2 & s_{NL} & s_{NL}^2 & 0 \\ 0 & 0 & 0 & 0 & 0 \end{pmatrix}$$

$$\langle x | \hat{O}_L | x' \rangle = \begin{pmatrix} 0 & 0 & 0 & 0 & 0 \\ 0 & s_L & 0 & 0 & 0 \\ 0 & 0 & 1 & 0 & 0 \\ 0 & 0 & 0 & s_L & 0 \\ 0 & 0 & 0 & 0 & 0 \end{pmatrix}$$

- here*: benchmark values for s_{NL} , s_L , $C_{0,2N}$ ($x = 2N$ coordinate difference in 1D)

- coefficients of “standard” CIs tuned to nucleon-nucleon phase shifts *

- PW decomposition using radial projection instead of Lüscher's formula)
 - Galilean-invariance restoration to correct deuteron binding energy for $\vec{P}_{tot} \neq \vec{0}$ *

Long-range interactions

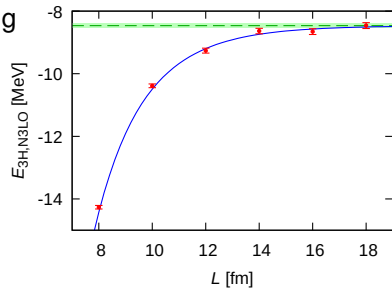
→ backup slide

Uncertainty analysis

- truncation error for observable X with zero external momentum:
 $\Delta X_{\text{trunc}}^{\text{NLO}} = \mathcal{Q}^3 |X_{\text{NLO}}|$, $\Delta X_{\text{trunc}}^{\text{N}^3\text{LO}} = \max\{\mathcal{Q}^5 |X_{\text{NLO}}|, \mathcal{Q}^2 |X_{\text{NLO}} - X_{\text{N}^3\text{LO}}|\}$
Epelbaum-Krebs-Meißner approach [EKM (2015a)] [EKM (2015b)] [N. Li et al. (2018)]
 - use N³LO without 3NF as NLO
 - estimate $\mathcal{Q} = M_\pi^{\text{eff}}/\Lambda_b = 200 \text{ MeV}/600 \text{ MeV} = 1/3$ [E. Epelbaum (2019)]

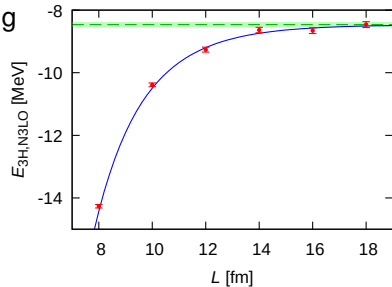
Uncertainty analysis

- truncation error for observable X with zero external momentum:
 $\Delta X_{\text{trunc}}^{\text{NLO}} = \mathcal{Q}^3 |X_{\text{NLO}}|$, $\Delta X_{\text{trunc}}^{\text{N}^3\text{LO}} = \max\{\mathcal{Q}^5 |X_{\text{NLO}}|, \mathcal{Q}^2 |X_{\text{NLO}} - X_{\text{N}^3\text{LO}}|\}$
Epelbaum-Krebs-Meißner approach [EKM (2015a)] [EKM (2015b)] [N. Li et al. (2018)]
 - use N³LO without 3NF as NLO
 - estimate $\mathcal{Q} = M_\pi^{\text{eff}}/\Lambda_b = 200 \text{ MeV}/600 \text{ MeV} = 1/3$ [E. Epelbaum (2019)]
- extrapolate binding energies E to $L \rightarrow \infty$ using suitable fit function $E(L)$:
$$E(L \rightarrow \infty) = E_\infty + E_0 L^{-3/2} \exp(-L/L_0)$$
 [Ulf-G. Meißner et al. (2015)]
 - propagate truncation error from data points to extrapolated result E_∞ via statistical sampling



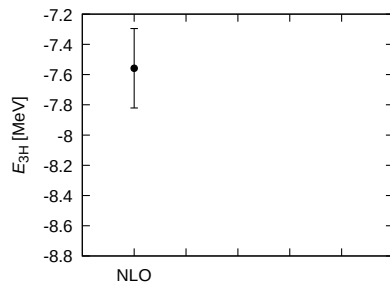
Uncertainty analysis

- truncation error for observable X with zero external momentum:
 $\Delta X_{\text{trunc}}^{\text{NLO}} = \mathcal{Q}^3 |X_{\text{NLO}}|$, $\Delta X_{\text{trunc}}^{\text{N}^3\text{LO}} = \max\{\mathcal{Q}^5 |X_{\text{NLO}}|, \mathcal{Q}^2 |X_{\text{NLO}} - X_{\text{N}^3\text{LO}}|\}$
Epelbaum-Krebs-Meißner approach [EKM (2015a)] [EKM (2015b)] [N. Li et al. (2018)]
 - use N³LO without 3NF as NLO
 - estimate $\mathcal{Q} = M_\pi^{\text{eff}}/\Lambda_b = 200 \text{ MeV}/600 \text{ MeV} = 1/3$ [E. Epelbaum (2019)]
- extrapolate binding energies E to $L \rightarrow \infty$ using suitable fit function $E(L)$:
$$E(L \rightarrow \infty) = E_\infty + E_0 L^{-3/2} \exp(-L/L_0)$$
 [Ulf-G. Meißner et al. (2015)]
 - propagate truncation error from data points to extrapolated result E_∞ via statistical sampling
- estimate fitting error from self-determined LEC $C \pm \Delta C$ as
$$\Delta X_{\text{fit}} = |X(C + \Delta C) - X(C - \Delta C)|/2$$
 - add truncation error and fitting error in quadrature: $\Delta X_{\text{tot}}^2 = \Delta X_{\text{trunc}}^2 + \Delta X_{\text{fit}}^2$



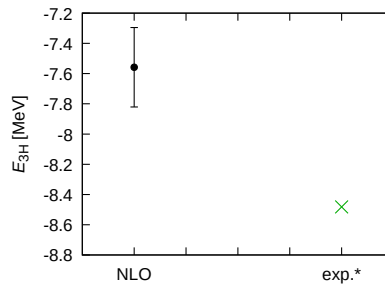
Binding energies

- lowest Hamiltonian eigenenergy from Lanczos alg. [C. Lanczos (1950)] [G. Stellin et al. (2018)]



Binding energies

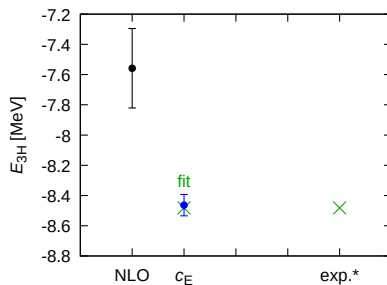
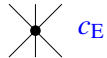
- lowest Hamiltonian eigenenergy from Lanczos alg. [C. Lanczos (1950)] [G. Stellin et al. (2018)]
- find LEC values $\{C, C - \Delta C, C + \Delta C\}$ that have E_{3H}^{exp} in truncation error bar



*[M. Wang et al. (2017)]

Binding energies

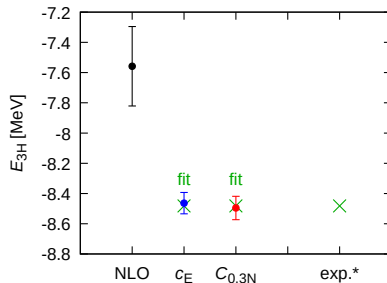
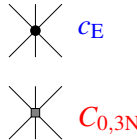
- lowest Hamiltonian eigenenergy from Lanczos alg. [C. Lanczos (1950)] [G. Stellin et al. (2018)]
- find LEC values $\{C, C - \Delta C, C + \Delta C\}$ that have E_{3H}^{exp} in truncation error bar
- $c_E = -0.398(8)$, $C_{0,3N} = c_D = 0$
⇒ three-nucleon contact interaction without smearing as in [D. Lee (2009)]



*[M. Wang et al. (2017)]

Binding energies

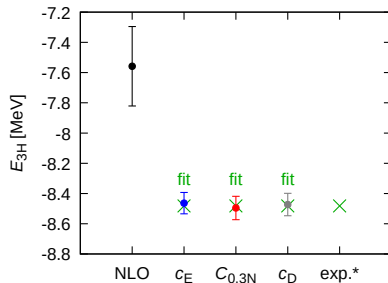
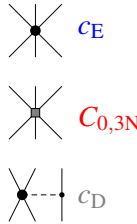
- lowest Hamiltonian eigenenergy from Lanczos alg. [C. Lanczos (1950)] [G. Stellin et al. (2018)]
- find LEC values $\{C, C - \Delta C, C + \Delta C\}$ that have E_{3H}^{exp} in truncation error bar
- $c_E = -0.398(8)$, $C_{0,3N} = c_D = 0$
⇒ three-nucleon contact interaction without smearing as in [D. Lee (2009)]
- $C_{0,3N} = -2.42(8) \times 10^{-12} \text{ MeV}^{-5}$, $c_E = c_D = 0$
⇒ 3N version of 2N SU(4)-invariant CI with non-local & local smearing



*[M. Wang et al. (2017)]

Binding energies

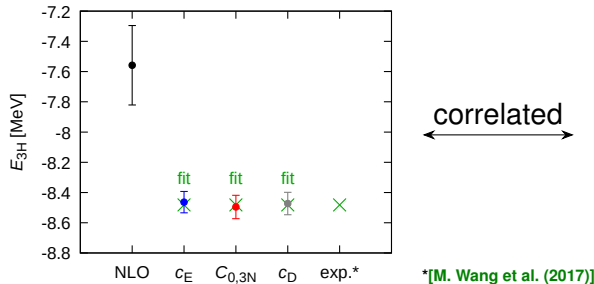
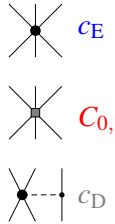
- lowest Hamiltonian eigenenergy from Lanczos alg. [C. Lanczos (1950)] [G. Stellin et al. (2018)]
- find LEC values $\{C, C - \Delta C, C + \Delta C\}$ that have E_{3H}^{exp} in truncation error bar
- $c_E = -0.398(8)$, $C_{0,3N} = c_D = 0$
⇒ three-nucleon contact interaction without smearing as in [D. Lee (2009)]
- $C_{0,3N} = -2.42(8) \times 10^{-12} \text{ MeV}^{-5}$, $c_E = c_D = 0$
⇒ 3N version of 2N SU(4)-invariant CI with non-local & local smearing
- $c_D = -5.16(16)$, $c_E = C_{0,3N} = 0$ ⇒ unsmeared 1π exchange



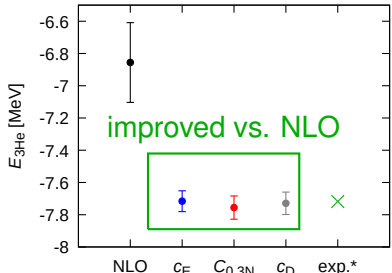
*[M. Wang et al. (2017)]

Binding energies

- lowest Hamiltonian eigenenergy from Lanczos alg. [C. Lanczos (1950)] [G. Stellin et al. (2018)]
- find LEC values $\{C, C - \Delta C, C + \Delta C\}$ that have E_{3H}^{exp} in truncation error bar
- $c_E = -0.398(8)$, $C_{0,3N} = c_D = 0$
⇒ three-nucleon contact interaction without smearing as in [D. Lee (2009)]
- $C_{0,3N} = -2.42(8) \times 10^{-12} \text{ MeV}^{-5}$, $c_E = c_D = 0$
⇒ 3N version of 2N SU(4)-invariant CI with non-local & local smearing
- $c_D = -5.16(16)$, $c_E = C_{0,3N} = 0$ ⇒ unsmeared 1π exchange



*[M. Wang et al. (2017)]



Charge radii

- charge radius: [J. Hoppe et al. (2019)] [J. Simonis et al. (2017)] [A. Ong et al. (2010)]

$$R_{\text{ch},\text{nucleus}}^2 = \langle \psi_{\text{nucleus}} | \hat{\vec{R}}_{\text{point-proton}}^2 | \psi_{\text{nucleus}} \rangle + R_{\text{ch,p}}^2 + \frac{N}{Z} R_{\text{ch,n}}^2 + R_{\text{Darwin-Foldy}}^2$$

with ground-state wave function ψ_{nucleus} for Z protons and N neutrons

Charge radii

- charge radius: [J. Hoppe et al. (2019)] [J. Simonis et al. (2017)] [A. Ong et al. (2010)]

$$R_{\text{ch},\text{nucleus}}^2 = \langle \psi_{\text{nucleus}} | \hat{\vec{R}}_{\text{point-proton}}^2 | \psi_{\text{nucleus}} \rangle + R_{\text{ch,p}}^2 + \frac{N}{Z} R_{\text{ch,n}}^2 + R_{\text{Darwin-Foldy}}^2$$

with ground-state wave function ψ_{nucleus} for Z protons and N neutrons

- determined ψ_{nucleus} for $L = 18$ fm using Lanczos algorithm

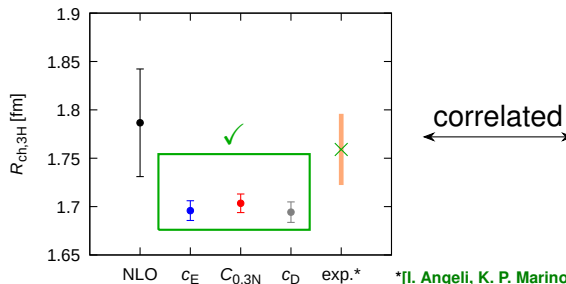
Charge radii

- charge radius: [J. Hoppe et al. (2019)] [J. Simonis et al. (2017)] [A. Ong et al. (2010)]

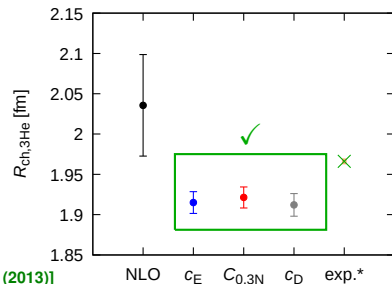
$$R_{\text{ch},\text{nucleus}}^2 = \langle \psi_{\text{nucleus}} | \hat{\vec{R}}_{\text{point-proton}}^2 | \psi_{\text{nucleus}} \rangle + R_{\text{ch,p}}^2 + \frac{N}{Z} R_{\text{ch,n}}^2 + R_{\text{Darwin-Foldy}}^2$$

with ground-state wave function ψ_{nucleus} for Z protons and N neutrons

- determined ψ_{nucleus} for $L = 18$ fm using Lanczos algorithm
- R_{ch} typically a few % too small (no hard repulsive core predicted in ChEFT)



*[I. Angeli, K. P. Marinova (2013)]



Half-life of triton beta decay

- half-life: [A. Baroni et al. (2016)] [R. Schiavilla et al. (1998)] [S. Raman et al. (1978)]

$$t_{1/2} = \frac{1}{1 + \delta_R} \frac{K/G_V^2}{f_V \langle \hat{\mathbf{F}} \rangle^2 + f_A g_A^2 \langle \hat{\mathbf{G}} \mathbf{T} \rangle^2}$$

Half-life of triton beta decay

- half-life: [A. Baroni et al. (2016)] [R. Schiavilla et al. (1998)] [S. Raman et al. (1978)]

$$t_{1/2} = \frac{1}{1 + \delta_R} \frac{K/G_V^2}{f_V \langle \hat{\mathbf{F}} \rangle^2 + f_A g_A^2 \langle \hat{\mathbf{G}} \mathbf{T} \rangle^2}$$

- Fermi and Gamow-Teller matrix elements for LO nuclear current:

$$\langle \hat{\mathbf{F}} \rangle = \sum_{n=1}^{N_{\text{nucleons}}} \langle \psi_{^3\text{He}} | \tau_{n,+} | \psi_{^3\text{H}} \rangle,$$

$$\langle \widehat{\mathbf{GT}} \rangle = \sum_{n=1}^{N_{\text{nucleons}}} \sqrt{3} \langle \psi_{^3\text{He}} | \tau_{n,+} \sigma_{n,z} | \psi_{^3\text{H}} \rangle = \text{Wavy Line} \bullet$$

diagram based on [H. Krebs et al. (2017)] using MUT

Half-life of triton beta decay

- half-life: [A. Baroni et al. (2016)] [R. Schiavilla et al. (1998)] [S. Raman et al. (1978)]

$$t_{1/2} = \frac{1}{1 + \delta_R} \frac{K/G_V^2}{f_V \langle \hat{\mathbf{F}} \rangle^2 + f_A g_A^2 \langle \hat{\mathbf{GT}} \rangle^2}$$

- Fermi and Gamow-Teller matrix elements for LO nuclear current:

$$\langle \hat{\mathbf{F}} \rangle = \sum_{n=1}^{N_{\text{nucleons}}} \langle \psi_{^3\text{He}} | \tau_{n,+} | \psi_{^3\text{H}} \rangle,$$

$$\langle \hat{\mathbf{GT}} \rangle = \sum_{n=1}^{N_{\text{nucleons}}} \sqrt{3} \langle \psi_{^3\text{He}} | \tau_{n,+} \sigma_{n,z} | \psi_{^3\text{H}} \rangle = \begin{array}{c} \text{W}^- \\ \diagdown \diagup \end{array}$$

diagram based on [H. Krebs et al. (2017)] using MUT

- determined $\psi_{^3\text{H}}$, $\psi_{^3\text{He}}$ for $L = 18$ fm
using Lanczos algorithm

Half-life of triton beta decay

- half-life: [A. Baroni et al. (2016)] [R. Schiavilla et al. (1998)] [S. Raman et al. (1978)]

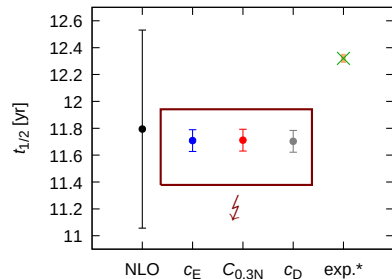
$$t_{1/2} = \frac{1}{1 + \delta_R} \frac{K/G_V^2}{f_V \langle \hat{\mathbf{F}} \rangle^2 + f_A g_A^2 \langle \hat{\mathbf{GT}} \rangle^2}$$

- Fermi and Gamow-Teller matrix elements for LO nuclear current:

$$\langle \hat{\mathbf{F}} \rangle = \sum_{n=1}^{N_{\text{nucleons}}} \langle \psi_{^3\text{He}} | \tau_{n,+} | \psi_{^3\text{H}} \rangle,$$
$$\langle \hat{\mathbf{GT}} \rangle = \sum_{n=1}^{N_{\text{nucleons}}} \sqrt{3} \langle \psi_{^3\text{He}} | \tau_{n,+} \sigma_{n,z} | \psi_{^3\text{H}} \rangle = \begin{array}{c} \text{W}^- \\ \sim \sim \sim \end{array} \mid$$

diagram based on [H. Krebs et al. (2017)] using MUT

- determined $\psi_{^3\text{H}}$, $\psi_{^3\text{He}}$ for $L = 18$ fm using Lanczos algorithm
- half-life too small with LO current (truncation error underestimated)



*[J. J. Simpson (1987)]

Summary and outlook

- good prediction for helion binding energy and charge radii of ^3H , ^3He

	$-E_{^3\text{H}}$ [MeV]	$-E_{^3\text{He}}$ [MeV]	$R_{\text{ch},^3\text{H}}$ [fm]	$R_{\text{ch},^3\text{He}}$ [fm]	$t_{1/2}$ [yr]
this work <small>c_E-fit</small>	8.46(7) <small>fit</small>	7.72(6)	1.6959(102)	1.9151(135)	
exp. <small>refs. on prev. slides</small>	8.481795(2)	7.718040(2)	1.7591(363)	1.9661(30)	12.32(3)

Summary and outlook

- good prediction for helion binding energy and charge radii of ^3H , ^3He
 - clear improvement by 3NF at N³LO compared to NLO (for fit of c_E , $C_{0,3\text{N}}$ and c_D)

	$-E_{^3\text{H}}$ [MeV]	$-E_{^3\text{He}}$ [MeV]	$R_{\text{ch},^3\text{H}}$ [fm]	$R_{\text{ch},^3\text{He}}$ [fm]	$t_{1/2}$ [yr]
this work <small>c_E-fit</small>	8.46(7) <small>fit</small>	7.72(6)	1.6959(102)	1.9151(135)	
exp. <small>refs. on prev. slides</small>	8.481795(2)	7.718040(2)	1.7591(363)	1.9661(30)	12.32(3)

Summary and outlook

- good prediction for helion binding energy and charge radii of ^3H , ^3He
 - clear improvement by 3NF at N³LO compared to NLO (for fit of c_E , $C_{0,3\text{N}}$ and c_D)
 - R_{ch} comparable to perturbative lattice ChEFT calculation with recent WFM potential [S. Elhatisari et al. (2024)]

	$-E_{^3\text{H}}$ [MeV]	$-E_{^3\text{He}}$ [MeV]	$R_{\text{ch},^3\text{H}}$ [fm]	$R_{\text{ch},^3\text{He}}$ [fm]	$t_{1/2}$ [yr]
WFM pot. <small>radii pert.</small>			1.7132(91)	1.9013(264)	
this work <small>c_E-fit</small>	8.46(7) <small>fit</small>	7.72(6)	1.6959(102)	1.9151(135)	
exp. <small>refs. on prev. slides</small>	8.481795(2)	7.718040(2)	1.7591(363)	1.9661(30)	12.32(3)

Summary and outlook

- good prediction for helion binding energy and charge radii of ^3H , ^3He
 - clear improvement by 3NF at N³LO compared to NLO (for fit of c_E , $C_{0,3\text{N}}$ and c_D)
 - R_{ch} comparable to perturbative lattice ChEFT calculation with recent WFM potential [S. Elhatisari et al. (2024)]
- non-pert. $t_{1/2}$ not improved by 3NF and slightly worse than for WFM potential [S. Elhatisari et al. (arXiv)]
⇒ consider $t_{1/2}$ (and $(\Delta t_{1/2})_{\text{trunc}}$) for N²LO current involving c_D [H. Krebs et al. (2017)]

	$-E_{^3\text{H}}$ [MeV]	$-E_{^3\text{He}}$ [MeV]	$R_{\text{ch},^3\text{H}}$ [fm]	$R_{\text{ch},^3\text{He}}$ [fm]	$t_{1/2}$ [yr]
WFM pot. <small>radii pert.</small>	8.33(2) <small>fit</small>	7.62(2)	1.7132(91)	1.9013(264)	12.095(2) <small>K/G_V^2</small>
this work <small>c_E-fit</small>	8.46(7) <small>fit</small>	7.72(6)	1.6959(102)	1.9151(135)	11.708(81)
exp. <small>refs. on prev. slides</small>	8.481795(2)	7.718040(2)	1.7591(363)	1.9661(30)	12.32(3)

Summary and outlook

- good prediction for helion binding energy and charge radii of ^3H , ^3He
 - clear improvement by 3NF at N³LO compared to NLO (for fit of c_E , $C_{0,3\text{N}}$ and c_D)
 - R_{ch} comparable to perturbative lattice ChEFT calculation with recent WFM potential [S. Elhatisari et al. (2024)]
- non-pert. $t_{1/2}$ not improved by 3NF and slightly worse than for WFM potential [S. Elhatisari et al. (arXiv)]
⇒ consider $t_{1/2}$ (and $(\Delta t_{1/2})_{\text{trunc}}$) for N²LO current involving c_D [H. Krebs et al. (2017)]
- outlook: test applicability of obtained potential to
 - nucleon-deuteron phase shifts using adiabatic projection method [M. Pine et al. (2013)]
 - perturbative calculations of heavier nuclei (bound states, resonances talk by C. Wang)

	$-E_{^3\text{H}}$ [MeV]	$-E_{^3\text{He}}$ [MeV]	$R_{\text{ch},^3\text{H}}$ [fm]	$R_{\text{ch},^3\text{He}}$ [fm]	$t_{1/2}$ [yr]
WFM pot. radii pert.	8.33(2) fit	7.62(2)	1.7132(91)	1.9013(264)	$12.095(2)_{K/G_V^2}$
this work c_E -fit	8.46(7) fit	7.72(6)	1.6959(102)	1.9151(135)	11.708(81)
exp. refs. on prev. slides	8.481795(2)	7.718040(2)	1.7591(363)	1.9661(30)	12.32(3)

Thank you for your attention!

Long-range interactions

- pion propagator with Gaussian regulator: [N. Li et al. (2018)]

$$\frac{1}{\vec{q}^2 + M_\pi^2} \exp\left(-\frac{\vec{q}^2 + M_\pi^2}{\Lambda^2}\right), \quad \Lambda = 200 \text{ MeV}$$

→ reduce Monte Carlo sign problem later [S. Elhatisari et al. (2024)]

- two-nucleon 1π exchange for M_{π^0} (isospin symmetric) and M_{π^0}, M_{π^\pm} (isospin breaking) [N. Li et al. (2018)]
- three-nucleon 1π exchange with unsmeared CI

as in [D. Lee (2009)] but not in [S. Elhatisari et al. (2024)]

→ LEC c_D fixed from triton binding energy

- three-nucleon double- 1π exchange [D. Lee (2009)] [S. Elhatisari et al. (2024)] with LECs c_1, c_3, c_4 adjusted to πN scattering data [M. Hoferichter et al. (2015)]
- Coulomb potential with zero particle distance replaced by $a/2$

[N. Li et al. (2018)]

